UNIVERSITY OF
BATH

University of Bath

Ultrashort Pulse Lossless Propagation Through a Degenerate Three-Level Medium in Nonlinear Optical Waveguides and Semiconductor Microcavities

Gabriela Slavcheva, John M. Arnold, and Richard W. Ziolkowski, *Fellow, IEEE*

Abstract—The authors develop and apply a novel group-theoretical approach for studying the coherent dynamics of ultrashort pulse propagation in nonlinear optical waveguides and passive semiconductor microresonators. The resonant nonlinearity is modeled by a degenerate three-level system of saturable absorbers in order to allow for a two-dimensional medium polarization. The resulting Maxwell-pseudospin equations are solved in the time domain using the finite-difference time-domain method. Conditions of onset of the self-induced transparency (SIT) regime of propagation are investigated. Numerical evidence of multidimensional solitons localized both in space and in time is given for the planar optical waveguides. Pattern formation and cavity SIT-soliton formation are demonstrated for a passive semiconductor microcavity filled with saturable absorbers.

Index Terms—Finite-difference time-domain (FDTD) method, light bullets, Maxwell–Bloch system, multidimensional solitons, resonant nonlinearities, self-induced transparency, semiconductor microcavities, spatiotemporal dynamics.

I. INTRODUCTION

CONTEMPORARY integrated optoelectronics and datacomm applications pose severe requirements on the stability of the shape of the propagating pulses as their temporal width is constantly decreased. As a consequence, the shorter the pulse is, the greater is the range of spectral components that it contains, and the greater is the tendency for the pulse to spread out during propagation. Therefore, dispersion presents a limit to either the shortness of the pulse or to the propagation distance without significant distortions in optical systems. A solution to this fundamental limitation might be sought either in engineering photonic structures, which would allow control of the pulse shape, or by introducing active resonant nonlinear media and exploiting the self-induced transparency effects in it, exploring and identifying lossless (soliton) regimes of propagation. It is more likely, however, that a combination of both approaches would provide a general solution in the future.

Since the pioneering work of McCall and Hahn [1], [2], it has been well known that the resonant coherent interaction of pulses shorter than the characteristic relaxation times of the medium gives rise to the effect of self-induced transparency (SIT) that results in solitary electromagnetic wave propagation

phenomena. Under the assumption of slow variation of all variables in space and time [slowly varying envelope approximation (SVEA)] and rotating wave approximation (RWA), the set of equations describing SIT is completely integrable in one dimension and the soliton solutions correspond to the 2π pulses [3]. It has been pointed out [4] that the SIT-soliton in one-dimensional (1-D) resonant medium is exponentially localized and stable. The original Maxwell–Bloch equations (without the restrictions of the SVEA and RWA) represent considerable interest since they provide a model of the resonant coherent interactions on ultrashort time scales. The analytical investigation of the full set of Maxwell–Bloch equations, however, is rather complex and no exact solutions have yet been found even in one dimension. If the restrictions of SVEA are removed and the requirement of unidirectional propagation is imposed, the so-called reduced Maxwell–Bloch equations are obtained, first derived by Eilbeck *et al.* [5]. It has been shown [6], [7] that the reduced set of Maxwell–Bloch equations in one dimension is an integrable system and consequently has soliton solutions. However, as has been pointed out in [8], the requirement of one-way wave propagation leads to a limitation of the resonant atoms' concentration. The assumption of one-way wave propagation neglects back scattering and, therefore, is applicable only at a relatively low dipole density, i.e., for resonant media composed of gases, metal vapors, or impurity doped glasses. Moreover, realistic situations require consideration of damping caused by dephasing processes and population relaxation, which in turn leads to additional terms in the Maxwell–Bloch system. This represents another complication for analytical methods. The basic limitations and oversimplifications of the analytical approaches can be overcome by employing various numerical techniques. In this respect, the efficiency of the finite-difference time-domain (FDTD) method, applied to the problem of ultrashort pulse interaction with a two-level atomic system in one dimension, has been demonstrated in [9].

The solution of the Maxwell–Bloch system and the related question of integrability become much more complicated in the more realistic multidimensional case. In this paper, we shall be interested in the novel, little investigated, class of multidimensional solitons, localized both in space and time, obtainable by two-dimensional (2-D) and three-dimensional (3-D) self-induced transparency phenomena which we shall call SIT-light bullets, in agreement with the terminology adopted for multidimensional spatial solitons [10], [11].

On the other hand, photonic structures, and in particular semiconductor microcavities containing resonant media, provide a uniquely advantageous combination of nonlinear properties that

allows for the existence of highly nonlinear modes of propagation. For example, the interplay between Bragg reflections that block the light propagation in photonic bandgaps, and the dynamical modifications of these reflections by coherent nonlinear light-matter interactions, results in a unique type of nonlinear modes, localized both in space and time, called cavity SIT-solitons. Cavity spatial solitons in semiconductor microresonators (light bullets) have been predicted in [12]. They have been a subject of intensive investigations by a number of theoretical and experimental groups in the past decade (for a recent review of the present state, see [13] and the references therein) in view of the possibility of realizing individually addressable pixel arrays based on SIT-cavity pattern formation effects. The latter can be exploited for optical storage of information and parallel optical processing utilizing the spatial solitons as fast mobile information carriers in a new type of information processing devices. However, for the sake of simplicity, these theoretical and numerical studies of the optical light bullets based on the Maxwell–Bloch system have always been limited to the slowly varying amplitudes of the electric field and polarization, or on the mean field approximation [12]. Here, we shall apply the novel formalism for description of the resonant coherent interactions of an optical wave with a discrete multilevel system, which has been previously developed and details of which have been published elsewhere [14].

In order to investigate the multidimensional spatiotemporal localization phenomenon, we need to consider at least a 2-D resonant medium. Generally, increasing the number of the spatial dimensions of the pulse propagation problem implies a corresponding increase in the number of the energy levels of the multilevel quantum system coupled to the electric field by dipole interaction. We have previously shown [14] that, as a minimum requirement, it is sufficient to consider a degenerate three-level ensemble of atoms in which two of the allowed electric dipole transitions are excited by each of the two components of the E-field in the waveguide plane. This allows for an adequate modeling of the interaction of an ultrashort laser pulse (one-photon excitation) with the medium in two spatial dimensions within the adopted generalized pseudospin formalism [15]. In what follows, we shall consider the most general case of a damped ensemble of dipole oscillators chosen as representative of a homogeneously broadened degenerate three-level quantum system of polarized atoms which is at or near resonance with the pulse of 2-D-wave radiation. This physical system could represent, for example, an ensemble of atomic dipoles enclosed in a small portion of a microcavity. However, the model potentially could represent an adequate description of the heavy-hole exciton transition in a quantum well within the two-band formulation for the semiconductors. The multisubband structure of such excitons is a motivation for applying the present model to the semiconductor quantum-well systems at the center of the Brillouin zone.

In this paper, we shall be aiming to give numerical evidence for the existence of 2-D SIT-soliton solutions in planar optical waveguides and semiconductor microcavities.

II. THEORETICAL BACKGROUND AND NUMERICAL IMPLEMENTATION

We employ the formalism developed in [14]. Our considerations are based on the generalized pseudospin formalism introduced in [15] for treatment of the resonant coherent interactions of ultrashort light pulses with discrete-multilevel systems. This formalism is based on the group-theoretical treatment applied to intense-field electrodynamics. It has been demonstrated that the dynamics of the multilevel laser-atom interacting system at or near resonance exhibits the Gell–Mann SU(N) symmetry. Exploiting the group-symmetry properties of the interaction Hamiltonian, we have originally derived a self-consistent set of coupled curl Maxwell-pseudospin equations in two spatial dimensions and time for the nonlinear resonant medium modeled by an ensemble of degenerate three-level quantum absorbers. We consider a V-type degenerate three-level system of resonant dipoles for which, as we have shown in [14], the dipole moment operators along the propagation direction and transverse to it are orthogonal. We have justified the degenerate three-level system as a minimum requirement in order to describe polarization induced by the electromagnetic wave in two orthogonal directions in the waveguide plane. The pseudospin equations are phenomenologically extended to include relaxation effects by introducing nonuniform decay times corresponding to the various dipole transitions occurring in a three-level system. We shall be interested in the TM mode of the 2-D optical wave in a parallel mirror waveguide since this mode couples all three levels of the system and therefore is irreducible to the 1-D case treated in [9]. Maxwell pseudospin equations for the TM wave derived in [14] read

$$\frac{\partial H_x}{\partial t} = -\frac{1}{\mu}\frac{\partial E_z}{\partial y} + \frac{1}{\mu}\frac{\partial E_y}{\partial z}$$

$$\frac{\partial E_y}{\partial t} = \frac{1}{\varepsilon}\frac{\partial H_x}{\partial z} - \frac{1}{\varepsilon}\frac{\partial P_y}{\partial t} \tag{1}$$

$$\frac{\partial E_z}{\partial t} = -\frac{1}{\varepsilon}\frac{\partial H_x}{\partial y} - \frac{1}{\varepsilon}\frac{\partial P_z}{\partial t}$$

$$P_y = -\wp N_a S_1; \quad P_z = -\wp N_a S_3 \tag{2}$$

$$\frac{\partial \mathbf{S}}{\partial t} = \mathbf{M}^{\mathrm{TM}}\mathbf{S} - \boldsymbol{\sigma}(\mathbf{S} - \mathbf{S_E}) \tag{3}$$

where $\mathbf{S}$ is an eight-dimensional real coherence vector describing the time evolution of the quantum system. The introduction of a real coherence (pseudospin) Bloch vector represents a generalization of the well known real-vector representation of the density matrix formalism for a two-level system. The real pseudospin vector components are related to the elements of the density matrix by the following:

$$S_1 = \hat{\rho}_{12} + \hat{\rho}_{21}; \quad S_2 = \hat{\rho}_{23} + \hat{\rho}_{32} \tag{4}$$

$$S_3 = \hat{\rho}_{13} + \hat{\rho}_{31}; \quad S_4 = -i(\hat{\rho}_{12} - \hat{\rho}_{21}) \tag{5}$$

$$S_5 = -i(\hat{\rho}_{23} - \hat{\rho}_{32}); \quad S_6 = -i(\hat{\rho}_{13} - \hat{\rho}_{31}) \tag{6}$$

$$S_7 = -(\hat{\rho}_{11} - \hat{\rho}_{22}); \quad S_8 = -\frac{1}{\sqrt{3}}(\hat{\rho}_{11} + \hat{\rho}_{22} - 2\hat{\rho}_{33}). \tag{7}$$

The physical meaning of the real coherence vector components is as follows: S_1 and S_4 represent, respectively, the dispersive or in-phase and the absorptive or in-quadrature polarization components associated with the dipole transition $1 \rightarrow 2$, S_2 and S_5 are the polarization components associated with the dipole transition $2 \rightarrow 3$, S_3 and S_6 are the polarization components associated with the dipole transition $1 \rightarrow 3$, and the last two

components S_7 and S_8 are the population terms representing the fractional population difference in a three-level system.

The matrix M^{TM} is 8×8 and antisymmetric with only nine independent nonvanishing components, given by

$$M^{TM} = \begin{pmatrix} 0 & 0 & 0 & -\omega_0 & -\Omega_z & 0 & 0 & 0 \\ 0 & 0 & 0 & \Omega_z & 0 & \Omega_y & 0 & 0 \\ 0 & 0 & 0 & 0 & \Omega_y & -\omega_0 & 0 & 0 \\ \omega_0 & -\Omega_z & 0 & 0 & 0 & 0 & -2\Omega_y & 0 \\ \Omega_z & 0 & 0 & -\Omega_y & 0 & 0 & 0 & 0 \\ 0 & -\Omega_y & \omega_0 & 0 & 0 & 0 & -\Omega_z & -\sqrt{3}\Omega_z \\ 0 & 0 & 0 & 2\Omega_y & 0 & \Omega_z & 0 & 0 \\ 0 & 0 & 0 & 0 & 0 & \sqrt{3}\Omega_z & 0 & 0 \end{pmatrix}. \tag{8}$$

We have defined Rabi frequencies of oscillations along the y and z directions according to

$$\begin{aligned} \Omega_y &= \frac{\wp}{\hbar} E_y \\ \Omega_z &= \frac{\wp}{\hbar} E_z \end{aligned} \tag{9}$$

where $\wp = eq_0$ is the dipole coupling constant and q_0 is a measure of the separation between the charges in the dipole. We have denoted the density of the resonant dipoles by N_a in (2) and in (3) introduced the diagonal matrix σ of the nonuniform relaxation rates of the eight components of the coherence vector $\mathbf{S}$ toward its equilibrium state $\mathbf{S_E}$

$$\sigma = \mathrm{diag}\left(\frac{1}{T_1}, \frac{1}{T_2}, \ldots, \frac{1}{T_8}\right). \tag{10}$$

Due to dephasing, only the last two population components of $\mathbf{S_E}$ are nonvanishing, namely $\mathbf{S_{7E}} = \pm 1$ and $\mathbf{S_{8E}} = \pm(1/\sqrt{3})$ in agreement with the normalization of the density matrix components. The equilibrium population terms define the initial population profile of the degenerate three-level system. We shall assume that $(-)$ corresponds to a system which is initially in its ground state and $(+)$ to the system with population inversion created by some pumping process, i.e., initially in the excited (doubly degenerate) upper state. Thus, we can model both absorbing and gain resonant media.

The full-wave vector Maxwell's equations coupled to the time evolution equations of the degenerate three-level quantum system are discretized using finite differences on a specially constructed modified Yee grid (Fig. 1) and solved numerically in the time domain using FDTD method [16]. This, in turn, allows a very general treatment which accounts for the nonlinearity, dispersion, absorption/amplification, saturation, and resonant effects without invoking any standard approximations (such as SVEA and RWA). We shall be interested in planar optical waveguide and semiconductor microcavity geometries (Fig. 2). The initial value problem considered is a Goursat-type one and, therefore, is well posed if the whole time history of the initial electric field is given along some characteristic (e.g., the beginning of the medium $z = 0$) (see [17]). We start to propagate a source pulse through the medium and monitor the spatiotemporal dynamics across the structure. We selected the guided modes of a parallel mirror waveguide as the most natural choice of the source field for the planar geometries under
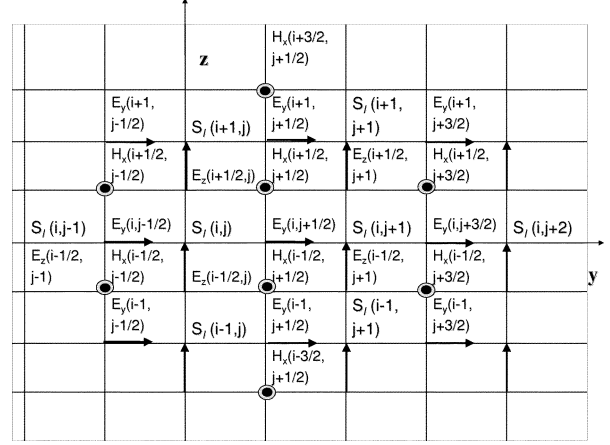

Fig. 1. Discretization of the Maxwell-pseudospin system using finite differences on a 2-D Yee grid with polarization variables S_j assigned to the empty nodes.
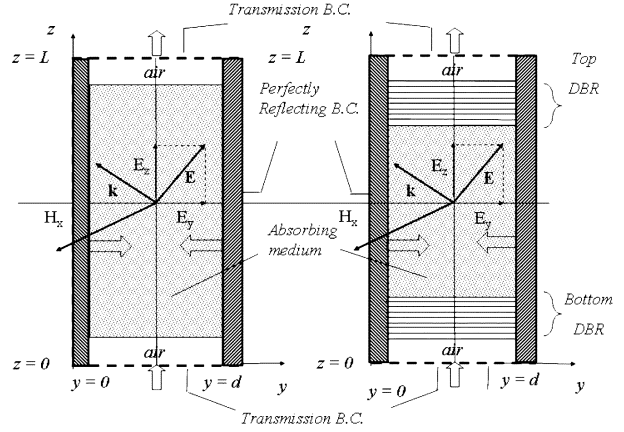

Fig. 2. Planar parallel mirror optical waveguide geometry (left), a semiconductor microcavity (right), and electromagnetic field configuration of the TM mode considered. Lower ($z = 0$) and upper ($z = L$) interfaces are perfectly transmitting, while the side walls are perfectly reflecting. Initially, the optical wave enters in the air buffer (free-space region) and afterwards propagates in the absorbing medium and exits through another free-space region; cavity is filled with absorbing medium in the case of semiconductor microcavity.

consideration. Initially, we apply the plane polarized TEM (or TM_0) mode with amplitude E_0, carrier frequency ω_0 tuned at the resonance of the degenerate three-level system, modulated by an arbitrary envelope. We conjecture a hyperbolic-secant (*h.s.*) envelope in two dimensions, as this is the stable solution envelope in 1-D self-induced transparency [1], [2]. Therefore, for any time moment, the initial pulse is given by

$$\begin{aligned} E_y(z=0,y,t) &= E_0 \,\mathrm{sech}(10\Gamma)\sin(\omega_0 t) \\ E_z(z=0,y,t) &= 0 \end{aligned} \tag{11}$$

where $\Gamma = [t - (T_p/2)]/(T_p/2)$ and T_p is the pulse duration. In the more general TM case, we excite a TM guided mode (e.g., TM_1) modulated by *h.s* envelope

$$\begin{aligned} E_y(z=0,y,t) &= E_0 c_1 \cos\left(\frac{\pi y}{d}\right)\mathrm{sech}(10\Gamma)\sin(\omega_0 t) \\ E_z(z=0,y,t) &= -E_0 c_2 \sin\left(\frac{\pi y}{d}\right)\mathrm{sech}(10\Gamma)\sin(\omega_0 t) \end{aligned} \tag{12}$$

with coefficients given by

$$c_1 = \frac{\sqrt{\frac{\omega_0^2 n^2}{c_0^2} - \left(\frac{\pi}{d}\right)^2}}{\omega_0 \varepsilon_0 n^2}; \quad c_2 = \frac{\frac{\pi}{d}}{\omega_0 \varepsilon_0 n^2} \tag{13}$$

where d is the separation between the mirrors and n is the refractive index of the medium between the mirrors, which in the case of a microcavity varies with the axial distance from the lower interface as the wave propagates through the multilayer system. Throughout the computations, we have imposed absorbing (perfectly transmitting) boundary conditions at the interfaces $z = 0$ and $z = L$ based on the Engquist–Majda one-way wave equation, derived in [14] and perfectly reflecting (perfectly conducting) boundary conditions on the side walls of the waveguide, i.e., $E_{\tan} = E_z = 0$. To ensure stability of the numerical algorithm, the time step is chosen according to the Courant stability criterion in two dimensions. The system (1)–(3) [with (8)–(10)] is solved by the FDTD time stepping algorithm with a predictor-corrector iterative scheme at each time step (see [14, Appendix]).

III. SIMULATION RESULTS

A. Planar Parallel-Mirror Optical Waveguides Filled With Absorbing Medium

We have thoroughly investigated the SIT phenomenon in two spatial dimensions in order to identify regimes of stable solitary wave propagation. As a validation study of the model, initially we have demonstrated soliton-like behavior of the plane-polarized TEM mode of a planar parallel mirror optical waveguide containing a resonantly absorbing medium (left part of Fig. 2). In particular, we show that if the initial pulse area of the pulse injected in the resonant absorbing medium $\theta_{\text{pulse}} = 2\pi$, the 2-D pulse continues to propagate undistorted, as predicted by the pulse area theorem [1], [2] for 1-D self-induced transparency solitons. We excite a $T_p = 100$ fs pulse from the lower boundary, whose maximum field amplitude is chosen according to the pulse area theorem, namely for a h.s.-modulated 2π pulse [14]

$$E_0 = \frac{2\pi \hbar f_0}{\wp \arctan(\sinh(u))\big|_{-10}^{10}}. \tag{14}$$

We assume the following values of the parameters in our simulations: excitation wavelength $\lambda = 1.5$ μm, corresponding to a frequency $f_0 = 2.0 \times 10^{14}$ s^{-1}, coupling coefficient $\wp = 1.0 \times 10^{-29}$ cm, number of resonant dipoles per unit volume $N_a = 10^{24}$ m^{-3}, and uniform relaxation times $T_1 = T_2 = \ldots T_8 = 1.0 \times 10^{-10}$ s $\gg T_p$ in order to satisfy the SIT criterion and to avoid virtual pulse distortions due to nonuniform decay rates. With this choice of parameters, the maximum pulse amplitude is $E_0 = 4.2186 \times 10^9$ Vm^{-1}. The following space and time steps are assumed in the simulations: $\Delta z = 30$ nm, $\Delta y = 300$ nm, $\Delta t = 9.989 \times 10^{-2}$ fs. In Fig. 3, we plot the time evolution of the stable soliton solution for the E_y field component along with the corresponding population term S_7 as compared with the dispersion case obtained for initial pulse area $\theta_{\text{pulse}} = 0.9\pi$, yielding maximum field amplitude $E_0 = 1.18957 \times 10^9$ Vm^{-1}. The comparison clearly shows
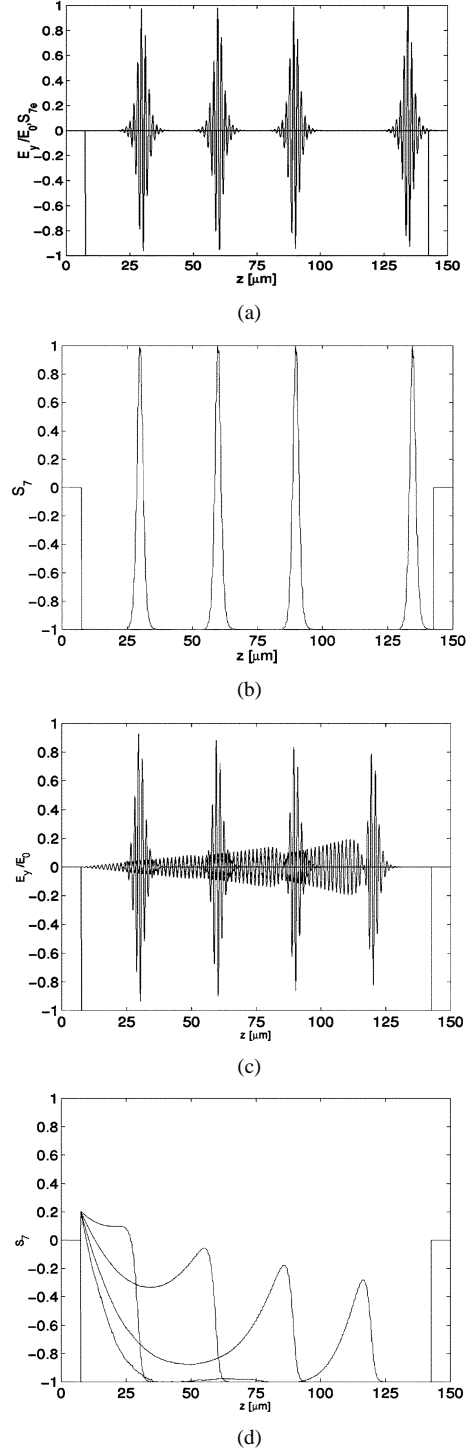

Fig. 3. Comparison between the soliton case (a), (b) and dispersion case (c), (d). (a) Longitudinal cross-section plot of the normalized component E_y of a 2π pulse. (b) Corresponding population inversion S_7 versus distance along the structure at the time $t = 150, 250, 350, 500$ fs; initial population profile S_{7e} indicates the boundaries of the absorbing medium. (c) Plot of the normalized component E_y of a 0.9π pulse. (d) Corresponding population inversion S_7 versus distance at the simulation times of (a), (b).

the increasing asymmetry of the pulse in the latter case, as the pulse continues to propagate through the absorbing medium. At the same time, the three-level system is only partially inverted and the population term does not exhibit full Rabi flopping, as in the soliton case. The energy absorbed by stimu-
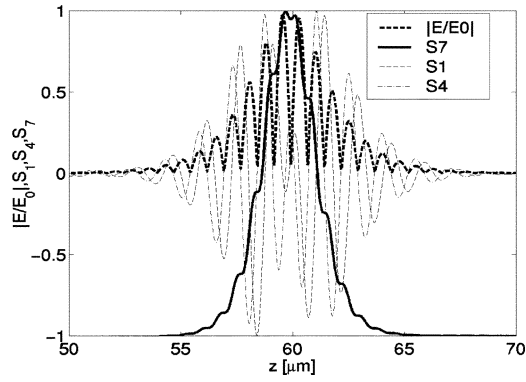
Fig. 4. Longitudinal cross section of the modulus of the electric field pulse and the meaningful real coherence vector components S_1, S_4, and S_7 representing the dispersive (in-phase) part of the induced medium polarization, the absorptive (in-quadrature) polarization component, and the Rabi flop of the population difference in the degenerate three-level system, respectively, for the soliton case of Fig. 3(a).

lated absorption during the initial fraction of the pulse gradually decreases, while at the same time the energy returned back to the electromagnetic field by stimulated emission increases, thus driving the pulse out of its initial equilibrium symmetric shape. This process persists until the leading edge of the pulse is fully absorbed and the trailing edge is emitted through the lower boundary. By contrast, in the soliton case (a), the pulse maintains its fully symmetric shape, thus propagating without losses through the absorbing medium. We demonstrate numerically the equivalence of the plane-polarized TEM mode propagation with the 1-D TE-soliton propagation considered in [9]. The real coherence vector components which have physical meaning in this case are plotted in Fig. 4 along with the electric field excitation for the soliton case [Fig. 3(a)]. Furthermore, we show that the TM_1 guided mode of the planar parallel-mirror waveguide which couples all three levels of the quantum system and, therefore, is irreducible to the 1-D case, exhibits soliton-like behavior, if the pulse amplitude satisfies a generalized pulse area theorem, which we have restated for the mutidimensional pulse propagation [14]. We show that if the initial pulse area below the field modulus is chosen as an even multiple of π, the solution obtained is stable and propagates without distortions in the absorbing medium. We launch a source field given by (12) and (13) corresponding to the TM_1 guided mode of the waveguide. The maximum pulse amplitude is calculated according to the generalized pulse area theorem, giving $E_0 = 1.123 \times 10^7$ Vm^{-1}. Spatial steps along the propagation axis z are chosen $\Delta z = 1.5$ nm, and $\Delta y = 119.5$ nm in the transverse direction, implying a time step $\Delta t = 5 \times 10^{-3}$ fs. The separation between the mirrors is taken as $d = 9.92$ μm and the refractive index is assumed to be $n = 1$. In Fig. 5, the time evolution of a 2π (in the sense of the generalized pulse area theorem) TM_1 pulse is plotted at three simulation times during the propagation in the absorbing medium together with the corresponding population inversion dynamics. The soliton-like behavior is clearly discerned from Fig. 5(a) and (b), showing unchanged pulse shape as the pulse travels through the absorbing medium, whose boundaries are indicated by the initial population profile S_{7E}. The population inversion [Fig. 5(c)] performs two Rabi flops across the transverse dimension of the optical waveguide due to the symmetry with
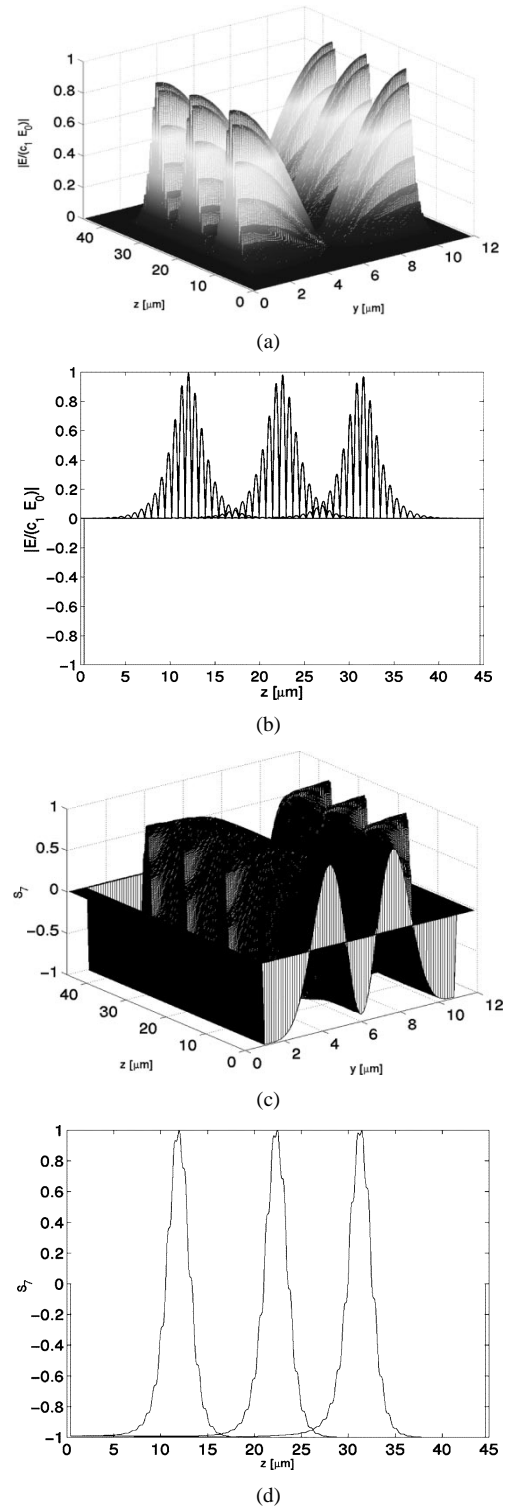

(a)

(b)

(c)

(d)

Fig. 5. (a) 3-D plot of the time evolution of the optical field of the TM_1 pulse modulus at the simulation times $t = 90, 125, 155$ fs. (b) Longitudinal cross section of (a) at the same simulation times. (c) 3-D-plot of the population inversion term S_7 time evolution corresponding to (a). (d) Longitudinal cross-section plot of (c).

respect to the propagation axis. The longitudinal Rabi flopping is plotted in Fig. 5(d) showing the same behavior of excitation to the upper doubly degenerate level and de-excitation back to the ground state caused by the pulse passage. Moreover, the characteristic cubic polynomial features are also present as in the previous case (compare with Fig. 4 and [9]).
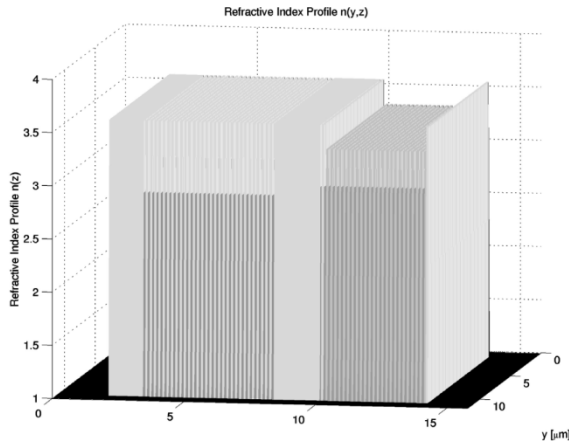
Fig. 6. 3-D-plot of the refractive index variation across the structure; cavity is filled with absorbing medium.

## B. Semiconductor Microcavities Filled With Absorbing Medium

We have investigated numerically conditions of onset of SIT-cavity soliton formation in a semiconductor microcavity driven by a coherent ultrashort pulse, applied at the lower boundary (Fig. 2, right). In order to test the influence of the cavity length on the patterns, we have designed a number of 2-D semiconductor microcavity geometries at an operating wavelength $\lambda = 1.3$ μm. The first microcavity geometry considered is composed of a $9\lambda/2$ cavity filled with absorbing medium ($S_{7E} = -1$; $S_{8E} = -1/\sqrt{3}$ initial population difference is assumed) embedded between 31.5 pairs GaAs/AlAs quarter-lambda layers [bottom distributed Bragg reflector (DBR)] and 24 pairs $Al_{0.5}Ga_{0.5}As/Al_{0.8}Ga_{0.2}As$ top DBR stacks preceded by an intermediate layer $Al_{0.8}Ga_{0.2}As/GaAs$. The refractive index profile as a function of the in-plane coordinates corresponding to the above structure is plotted in Fig. 6. Initially, an ultrashort plane-wave (TEM) pulse $T_p = 10$ fs is excited from the lower interface (Fig. 2 right-hand side, or Fig. 6 ($z = 0$)), at the atomic resonance carrier frequency, modulated by a hyperbolic secant as a trial pulse. The choice of the envelope is assumed consistent with the waveguide soliton solutions. The maximum pulse amplitude is calculated according to the pulse area theorem, leading to a value of $E_0 = 3.891\,44 \times 10^{10}$ Vm^{-1}. The relaxation times are kept uniform and equal to 100 ps throughout the simulations in order to satisfy the SIT criterion and to avoid any distortions that may occur due to the different time scales of the decoherence processes. The dipole density and the dipole coupling constant are chosen in agreement with the previous section, respectively, as $N_a = 10^{24}$ m^{-3} and $\wp = 1.0 \times 10^{-29}$ cm. The width of the microcavity between the side mirrors is chosen the same as in the waveguide case, namely $d = 9.92$ μm. In what follows, we shall show that the pulse area requirement is not a necessary condition in order to obtain SIT cavity patterns. Similar to the self-induced transparency in resonantly absorbing Bragg reflectors (RABR) the initial pulse may have an arbitrary pulse area [18]–[21]. Even relatively weak pulse amplitudes would lead to SIT intracavity patterns after sufficiently long simulation times. We shall be interested in the intracavity pattern formation dynamics. In Figs. 7 and 8, examples of the
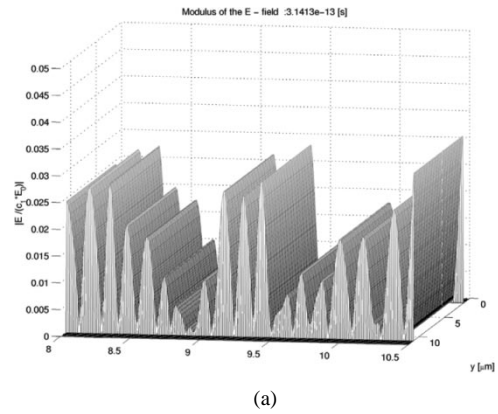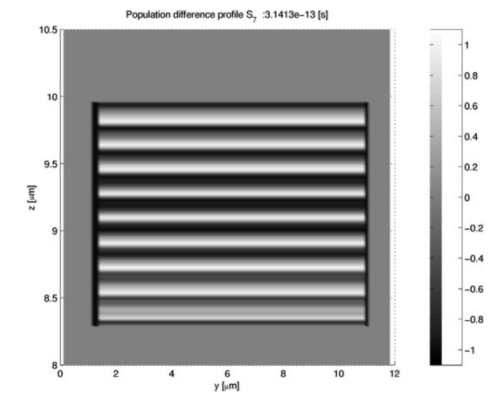

(a)
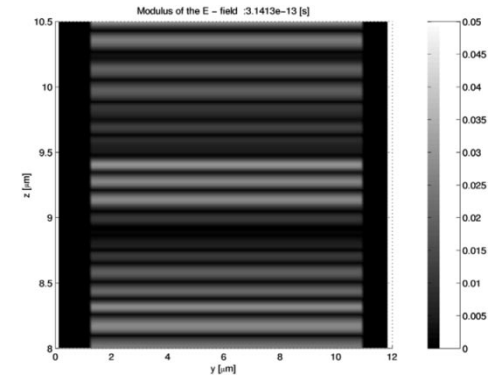
(b)
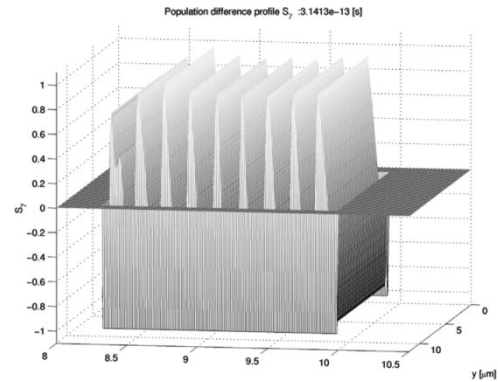
(c)

(d)

Fig. 7. (a) 3-D-plots of the modulus of the electric field in the vicinity of the microcavity. (b) Top view of the modulus of the electric field. (c) 3-D-plot of the population inversion quasi-stationary pattern induced in the cavity. (d) Population inversion roll patterns (top view).
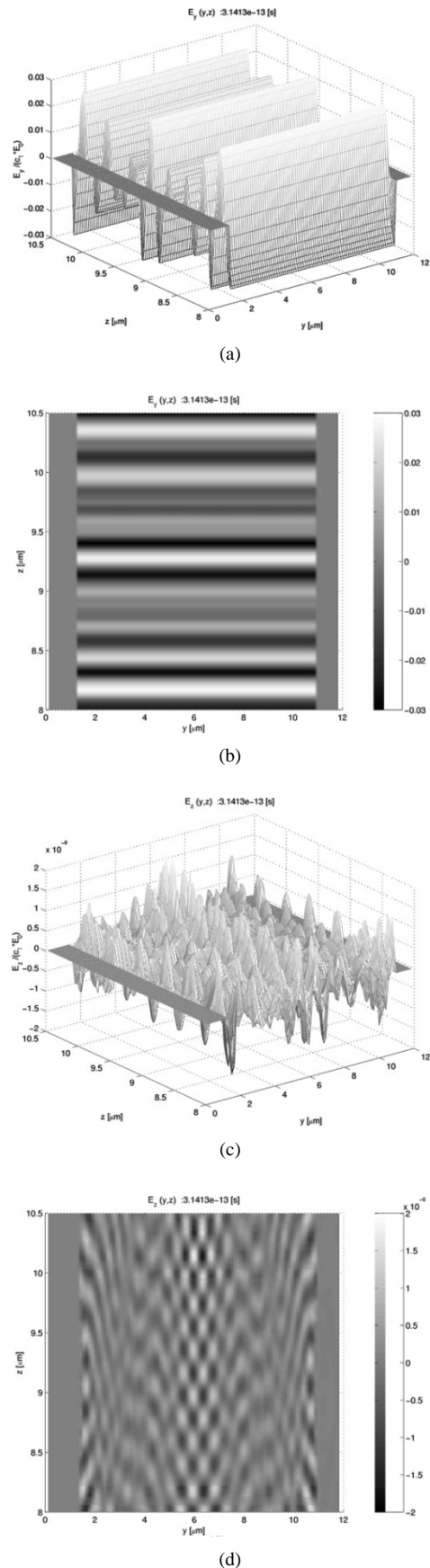
(a)

(b)

(c)

(d)

Fig. 8. (a) 3-D-plots of the E_y electric field component in the vicinity of the microcavity. (b) Top view of the E_y electric field component distribution. (c) 3-D-plot of the E_z component. (d) Top view of the spatial pattern of the E_z field component.

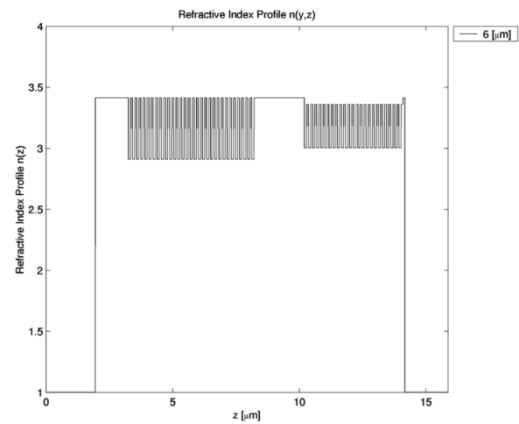

Fig. 9. Longitudinal cross section of the refractive index profile at a distance 6 μm from the left interface.

quasi-stationary periodic patterns found are plotted. Localized electric field modulus (or, equivalently electric field intensity) roll patterns are observed within the cavity (see top line of Fig. 7), giving rise to a specific number of full Rabi flops of the population from the ground state with initial population profile $S_7 = -1$ to the upper degenerate level with population profile $S_7 = +1$, returning the population back to the ground state. Note that the number of full Rabi flops performed within the cavity is exactly equal to the number of the half-wavelengths across the cavity length (nine in this case, since the cavity length has been chosen $L_c = (9\lambda)/(2n)$. Although the amplitude of the field intensity is changed with time, the number of the maxima within the cavity corresponds to the number of the Rabi flops in the level population occupancy, thus forming a population inversion grating. The electric field pattern and the population roll pattern exhibit the features of quasi-stationary standing wave (quiescent) SIT-soliton. The population Rabi flopping inside the cavity gradually builds up with time starting from only a partially inverted system to ultimately a completely inverted system (or very close to it), as shown in Fig. 7(c) and (d). The combined effect of the multiple reflections from the Bragg mirrors and the cavity length of the Fabry–Pérot resonator (chosen as a multiple of the dielectric half-wavelength) enhances the coupling between the driving electromagnetic field and the three-level absorbing medium, thus resulting in electric field localization (standing wave) and at the same time causing Rabi flops of the population inversion at the antinodes of the quasi-stationary standing wave. In fact, this situation is reminiscent of the continuous wave formation of a standing wave profile along the cavity. However, the continuous wave amplitude is not sufficient to invert locally the system. This can be achieved by an ultrashort pulse excitation with sufficiently high intensity. At the same time, roll patterns and more complicated ones are observed for the E_y and E_z field component, as can been from Fig. 8(a)–(d).

In order to test out the hypothesis of the existence of a unique type of SIT nonlinear mode inside the cavity, we have performed simulations on a number of different designs and driving pulse durations. In particular, we have designed a structure operating at $\lambda = 1.3 \, \mu$m shown in Fig. 9.

The semiconductor microresonator consists of two Bragg mirrors, GaAs/AlAs (31.5 pairs), and $Al_{0.1}Ga_{0.9}As/$
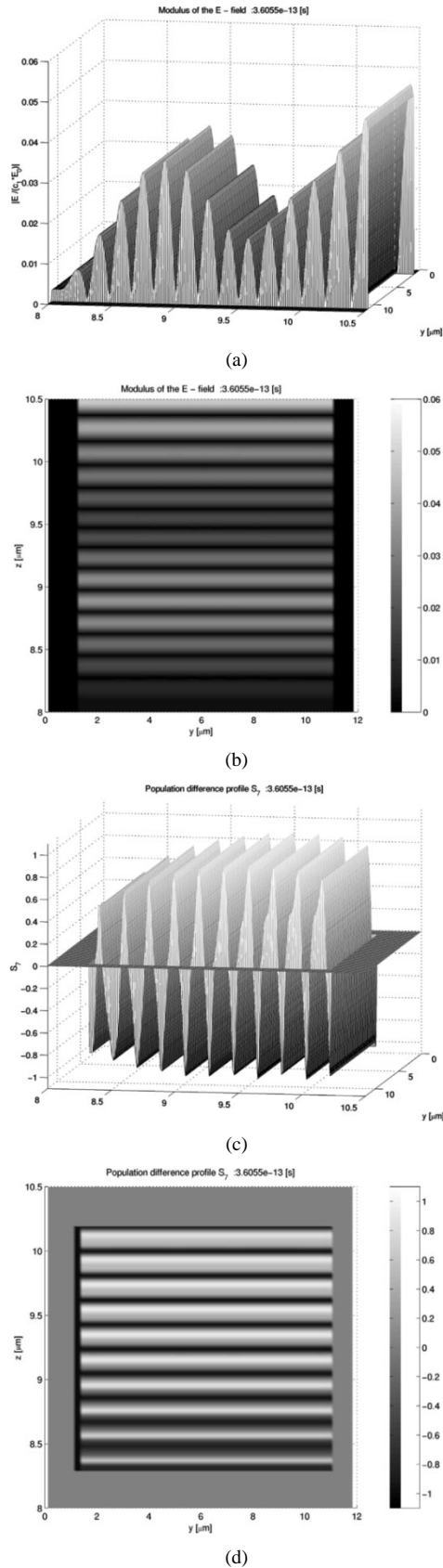
(a)

(b)

(c)

(d)

Fig. 10.   (a) 3-D-plots of the E-field modulus. (b) Top view of (a) showing the roll patterns formed. (c) 3-D-plot of the corresponding population inversion S_7 in the cavity. (d) Top views of (c) showing the roll patterns formed.

$Al_{0.8}Ga_{0.2}As$ (24 pairs), respectively, for the bottom and top DBR, and a $((5\lambda)/n)$ cavity. We apply a driving pulse
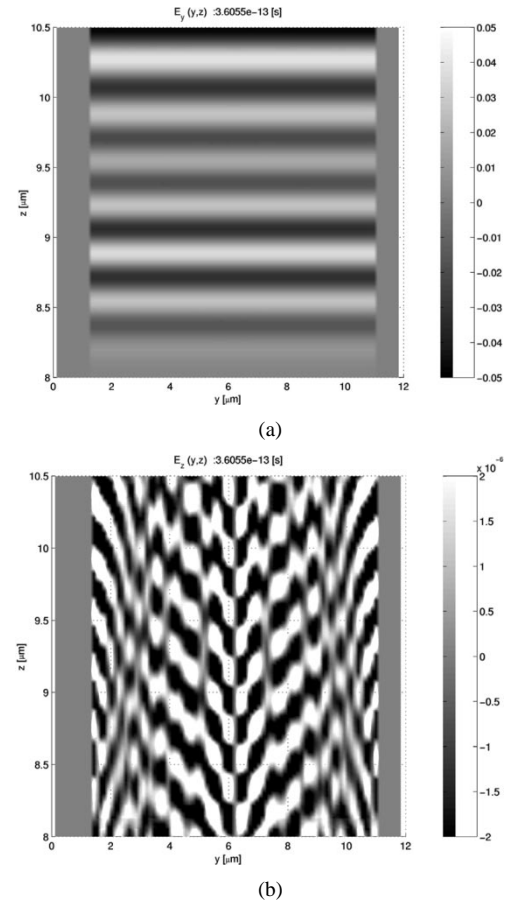

(a)

(b)

Fig. 11.   (a) Top view of the E_y field component in the vicinity of the cavity. (b) Top view of the E_z field component showing a complex pattern.

excitation with duration $T_p = 100$ fs, which results in a maximum field amplitude of $E_0 = 4.8643 \times 10^9$ Vm^{-1}, if the pulse area relationship is assumed to be still valid. In Fig. 10, the electric field modulus and the population inversion profile in the cavity are plotted. The roll patterns are evident both for the E-field and for the population inversion [Fig. 10(d)]. The number of half-wavelengths over the cavity length and the quasi-complete Rabi flops of the population is ten, i.e., exactly equal to the number of dielectric half-wavelengths contained within the cavity length $L_c = (10\lambda)/(2n)$ in agreement with the design parameter. This represents another confirmation of the positioning and the number of the maxima of the population grating induced by the cavity field. The respective E-field component patterns are shown in Fig. 11(a) and (b).

To summarize our simulation results for the semiconductor microcavities, we have demonstrated numerically on the basis of the Maxwell-pseudospin [(1)–(3) with (8)–(10)] the existence of a new type of a multidimensional spatiotemporally localized standing-wave "light bullet." The SIT-cavity quasi-soliton is a product of the interplay between the resonant nonlinearity of the atomic medium and the Bragg reflections in the Fabry–Pérot microresonator. Intuitively, we expect that the pulse area theorem does not apply for a multilayer (nonuniform) medium, since the pulse area is split between the forward and backward (reflected) propagating waves and is no longer conserved. However, even driving the cavity from outside the microresonator, applying sufficiently high initial pulse intensities (calculated on

the basis of the pulse area theorem in homogeneous medium), we could still compensate for the attenuation of the wave intensity due to the multiple back-reflections during the passage through the Bragg mirror, as the simulations show. It becomes apparent that the proper design of a high-finesse semiconductor microcavity geometry is crucial for the stability of the observed SIT cavity patterns.

IV. SUMMARY

In this paper, we employ the methodology of numerical FDTD solution of the full-wave vectorial Maxwell-pseudospin system to explore the conditions of onset of a self-induced transparency soliton regime of propagation in planar optical waveguides containing resonant nonlinearities and to predict a novel type of multidimensional SIT pattern formation in the semiconductor microcavities loaded with absorbing medium. We have successfully demonstrated self-induced transparency in two spatial dimensions in resonantly absorbing planar parallel mirror waveguides and generalized accordingly the pulse area theorem to the multidimensional case. Furthermore, we have extended the model to account for the multiple reflections in the multilayer DBR mirrors and applied it to the number of realistic geometries of semiconductor microcavities in two spatial dimensions. We have focused on the specific class of spatiotemporally localized multidimensional solitons predicted by the numerical computations which manifests itself by spatial pattern formation and a related grating of the population inversion. The advantage of the present approach is in capturing a full physical picture of the resonant coherent interactions beyond the limitations imposed by the slowly varying envelope and rotating wave approximations, thus enabling us to describe the spatiotemporal dynamics of the ultrashort pulse interactions. It is possible to implement within the adopted formalism the more realistic inhomogeneously broadened resonant line shape by introducing the appropriate resonant energy distribution function into the active medium. However, we expect that the inclusion of inhomogeneous broadening would not result in any dramatic changes of the SIT soliton-like behavior. We believe that a complete understanding of the design issues and the initial operative conditions is essential for the realization of devices based on the principles of the self-induced transparency.

ACKNOWLEDGMENT

REFERENCES

[1] S. L. McCall and E. L. Hahn, "Self-induced transparency," *Phys. Rev.*, vol. 183, pp. 457–485, 1969.
[2] ——, "Self-induced transparency by pulsed coherent light," *Phys. Rev. Lett.*, pp. 908–911, 1967.
[3] L. Allen and J. H. Eberly, *Optical Resonance and Two-Level Atoms*. New York: Wiley, 1975.
[4] A. I. Maimistov, A. M. Basharov, O. Elyutin, and Yu. M. Sklyarov, "Present state of self-induced transparency theory," *Phys. Rep.*, vol. 191, pp. 1–108, 1990.
[5] J. C. Eilbeck, J. D. Gibbon, P. J. Caudrey, and R. K. Bullough, *J. Phys. A: Math., Nucl. Gen.*, vol. 6, p. 1337, 1973.
[6] P. P. Goldstein, "Testing the Painlevé property of the Maxwell-Bloch and reduced Maxwell-Bloch equations," *Phys. Lett. A*, vol. 121, pp. 11–14, 1987.
[7] A. Grauel, "Optical networking update," *J. Phys. A*, vol. 19, pp. 479–779, 1986.
[8] R. K. Bullough, P. M. Jack, P. W. Kitchenside, and R. Saunders, "Solitons in laser physics," *Phys. Scr.*, vol. 20, pp. 364–381, 1979.
[9] R. W. Ziolkowski, J. M. Arnold, and D. M. Gogny, "Ultrafast pulse interactions with two-level atoms," *Phys. Rev. A*, vol. 52, pp. 3082–3094, 1995.
[10] Y. Silberberg, "Collapse of optical pulses," *Opt. Lett.*, vol. 15, pp. 1282–1284, 1990.
[11] M. Blaauboer, B. A. Malomed, and G. Kurizki, "Spatiotemporally localized multidimensional solitons in self-induced transparency media," *Phys. Rev. Lett.*, vol. 84, pp. 1906–1909, 2000.
[12] W. J. Firth and A. J. Scroggie, "Optical bullet holes: robust controllable localized states of a nonlinear cavity," *Phys. Rev. Lett.*, vol. 76, pp. 1623–1626, 1996.
[13] S. Barland, J. R. Tredicce, M. Brambilla, L. A. Lugiato, S. Balle, M. Guidici, T. Maggipinto, L. Spinelli, G. Tissoni, T. Knödl, M. Miller, and R. Jäger, "Cavity solitons as pixels in semiconductor microcavities," *Nature*, 2002.
[14] G. Slavcheva, J. M. Arnold, I. Wallace, and R. W. Ziolkowski, "Coupled Maxwell-pseudospin equations for investigation of self-induced transparency effects in a degenerate three-level quantum system in two dimensions: finite-difference time-domain study," *Phys. Rev. A*, vol. 66, p. 063 418, 2002.
[15] F. T. Hioe, "Dynamic symmetries in quantum electronics," *Phys. Rev. A*, vol. 28, pp. 879–886, 1983.
[16] A. Taflove, *Computational Electrodynamics: The Finite-Difference Time-Domain Method*. Norwood, MA: Artech, 1995.
[17] A. C. Newell and J. V. Moloney, *Nonlinear Optics*. Redwood City, CA: Addison-Wesley, 1992, p. 233.
[18] A. Kozhekin and G. Kurizki, "Self-induced transparency in Bragg reflectors: Gap solitons near absorption resonances," *Phys. Rev. Lett.*, vol. 74, pp. 5020–5023, 1995.
[19] A. Kozhekin, G. Kurizki, and B. Malomed, "Standing and moving gap solitons in resonantly absorbing gratings," *Phys. Rev. Lett.*, vol. 81, pp. 3647–3650, 1998.
[20] M. Blaauboer, G. Kurizki, and B. A. Malomed, "Spatiotemporally localized solitons in resonantly absorbing Bragg reflectors," *Phys. Rev. E*, vol. 62, pp. R57–R59, 2000.
[21] G. Kurizki, D. Petrosyan, T. Opratny, M. Blaauboer, and B. Malomed, "Self-induced transparency and giant nonlinearity in doped photonic crystals," *J. Opt. Soc. Amer. B*, vol. 19, pp. 2066–2074, 2002.

Gabriella Slavcheva received the M.Sc. degree in semiconductor physics from Sofia University, Sofia, Bulgaria, in 1983 and the Ph.D. degree in theoretical condensed matter physics from the Bulgarian Academy of Sciences, Sofia, Bulgaria, in 1997.

After graduation, she joined the Institute of Solid State Physics (BAS) as a Ph.D. student doing theoretical and experimental research on low-dimensional disordered semiconductor nanostructures. She spent subsequently three-and-a-half years leave in the Institute of Acoustics (C.N.R.), Rome, Italy, working on vibrational dynamics of semiconductor superlattices and inhomogeneous elastic membranes and a six-month leave at the Physics Department, Chulalongkorn University, Bangkok, Thailand, as a Visiting Professor, working on the path-integration methods applied to the electronic structure calculations of low-dimensional disordered semiconductors. In 1999, she joined the Device Modeling Group at the University of Glasgow, U.K. There she worked on a NASA project "Limits of miniaturization of Semiconductor Devices," developing theoretical methods for treatment of statistical fluctuations in sub-0.1–μm devices and quantum confinement effects, incorporated in the three-dimensional atomistic solver. In 2000, she joined the Optoelectronics Research Group. Her research interests include the development of a quantum electronics model for the nonlinear coherent dynamics in one and two dimensions and FDTD numerical implementation on a parallel multiprocessor server. Her research interests also include theoretical condensed matter physics, theoretical and computational quantum electronics, nonlinear optics, and high-performance computing. She has published more than 30 research articles in refereed journals and papers at international conferences.

John M. Arnold received the B.Eng. degree in electronic engineering and the Ph.D. degree from the University of Sheffield, U.K., in 1968 and 1974, respectively.

He was a Postdoctoral Research Assistant at the Department of Electronic and Electrical Engineering, Queen Mary College, University of London, London, U.K., from 1974 to 1978. In 1978, he was appointed Lecturer at the Department of Electronic and Electrical Engineering, University of Nottingham, U.K. In 1985, he was appointed Lecturer in the Department of Electronics and Electrical Engineering, University of Glasgow, U.K., where has been Professor of Applied Electromagnetics since 1994. He was appointed Head of Department of Electronics and Electrical Engineering in April 2003. His research interests include mathematical methods in applications to optics and electromagnetic wave propagation, particularly in nonlinear guided-wave optics and semiconductor lasers.

Dr. Arnold is a Fellow of the Institute of Physics. He is a Member of the URSI Commission B and has served as the U.K. National Representative for URSI Commission B from 1991 to 1996.

Richard W. Ziolkowski (M'87–SM'91–F'94) received the Sc.B. degree in physics *magna cum laude* from Brown University in 1974 and the M.S. and Ph.D. degrees in physics from the University of Illinois, Urbana-Champaign, in 1975 and 1980, respectively.

He was a Member of the Engineering Research Division at the Lawrence Livermore National Laboratory from 1981 to 1990 and served as the Leader of the Computational Electronics and Electromagnetics Thrust Area for the Engineering Directorate from 1984 to 1990. He joined the Department of Electrical and Computer Engineering at the University of Arizona, Tempe, as an Associate Professor in 1990, and was promoted to Full Professor in 1996. His research interests include the application of new mathematical and numerical methods to linear and nonlinear problems dealing with the interaction of acoustic and electromagnetic waves with realistic materials and structures.

Dr. Ziolkowski is a member of Tau Beta Pi, Sigma Xi, Phi Kappa Phi, the American Physical Society, the Optical Society of America, the Acoustical Society of America, and Commissions B (Fields and Waves) and D (Electronics and Photonics) of the International Union of Radio Science (URSI). He was an Associate Editor for the IEEE TRANSACTIONS ON ANTENNAS AND PROPAGATION from 1993 to 1998. He served as the Vice Chairman of the 1989 IEEE/AP-S and URSI Symposium in San Jose, CA, and as the Technical Program Chairperson for the 1998 IEEE Conference on Electromagnetic Field Computation in Tucson, AZ. He served as a member of the IEEE AP-S Administrative Committee (ADCOM) from 2000 to 2002. For the U.S. URSI Commission B, he served as Secretary from 1993 to 1996 and as Chairperson of the Technical Activities Committee from 1997 to 1999. He is currently serving as a Member-at-Large of the U.S. National Committee (USNC) of URSI and as Secretary for the U.S. URSI Commission D. He was a Co-Guest Editor of the 1998 special issue of *Journal of the Optical Society of America A*, featuring Mathematics and Modeling in Modern Optics. He was a Co-Organizer of the Photonics Nanostructures Special Symposia at the 1998, 1999, and 2000 OSA Integrated Photonics Research (IPR) Topical Meetings. He served as the Chair of the IPR subcommittee IV, Nanostructure Photonics, in 2001. He was awarded the Tau Beta Pi Professor of the Year Award in 1993 and the IEEE and Eta Kappa Nu Outstanding Teaching Award in 1993 and 1998.